Controlling the Growth of Conjugated Polymers on Electrode Surface: Synthesis, Electropolymerization, and Spectroelectrochemistry of Conjugated Bispyrroles

Michael Büschel,[†] Ayyappanpillai Ajayaghosh,*[,‡] Joby Eldo,[‡] and Jörg Daub*[,†]

Institut für Organische Chemie, Universität Regensburg, Universitätsstrasse 31, D-93040 Regensburg, Germany; and Photochemistry Research Unit, Regional Research Laboratory, CSIR, Trivandrum 695019, India

Received May 7, 2002; Revised Manuscript Received August 23, 2002

ABSTRACT: Fluorescent bispyrroles **6**−**9** consisting of different aromatic bridging moieties were prepared and characterized. Detailed studies on the electropolymerization, cyclic voltammetry, and spectroelectrochemistry are reported. The electronic character of the bridging moieties and the solubility inducing hydrocarbon side chains play crucial roles in controlling the growth of the polymer film on the electrode surface. The bispyrroles with divinylbenzene and divinylnaphthalene bridging groups react under film formation while the corresponding divinylanthracene-bridged bispyrrole show reversible formation of the dication $\mathbf{9}^{2+}$ exhibiting a "two-electron−one-wave" feature. Presence of alkoxy substituents on the divinylbenzene moiety is shown to have adverse effect on the electropolymerization. The role of the bridging moieties in controlling the film growth on the electrode surface is rationalized on the basis of the orbital coefficients at the C^{α}-positions of the pyrrole moieties, which in turn are determined by the electronic nature of the conjugation bridge.

Introduction

Conjugated organic materials are finding widespread application in the emerging area of electrooptical and photonic materials.[1] In this context, synthesis of π-conjugated oligomers and polymers are of special interest since they are amenable to structural modification and processing.[2] A crucial aspect of the designing of such materials is the tuning of their optical and electronic properties, which are usually achieved by the careful choice of monomers.[3] For example, incorporation of electron-donating or -withdrawing substituents can have an influence upon the energy levels of the highest occupied and the lowest unoccupied molecular orbitals of conjugated monomers, polymerization of which allows the modulation of electrical conductivity, light-emitting properties, and nonlinear optical (NLO) behavior.

Electropolymerization of heterocyclic monomers is an area of considerable importance due to the diverse applications of redox-active conducting polymers as electrochromic materials and as supercapacitors.[4,5] In this context, electropolymerization of pyrrole has been the subject of several studies.[6] When compared to many other conjugated polymers, polypyrrole exhibits high redox stability, high conductivity, and better electrochromic properties. Reports pertaining to the electropolymerization of oligopyrroles of different conjugation lengths are also available in the literature.[7] Apart from these studies, there are several reports devoted to the electropolymerization of structurally modified pyrrole derivatives.[8−13] For example, incorporation of electron-rich and electron-deficient conjugated bridging units are known to alter the electrochemical properties of bispyrroles.[8,9] Electropolymerization of such monomers to form redox-active conducting polymers is highly dependent upon the monomer's oxidation potential. Extension of conjugation in bispyrroles by means of aromatic and conjugated bridging units can induce significant reduction of the oxidation potentials. With such low oxidation potentials, the polymer will be quite stable as a conductor and can be subjected to a large number of redox cycles with minimal degradation in charge response.[9]

Recently we have reported the synthesis of 1,4-dialkoxydivinylbenzene-bridged bispyrroles, which show high fluorescence emission.[14] These monomers are ideal building blocks for the designing of a variety of conjugated oligomers and polymers as depicted in Figure 1. For example, recently we have demonstrated the use of a few of these electron rich bispyrroles for the synthesis of near-infrared absorbing polysquaraines having extremely low optical band gaps.[15] Herein we report the synthesis, electropolymerization, redox properties, and spectroelectrochemistry of a few fluorescent bispyrroles, **6**−**9** (Chart 1), which show distinctly different behaviors on an electrode surface upon potential cycling.

Results and Discussion

Synthesis and Spectroscopic Properties of the Monomers. The bispyrroles **6**−**9** were prepared according to Scheme 1. The bis(bromomethylaryl) derivatives used in the present study were obtained by standard procedures. The Michaelis Arbuzov reaction[16] of the bis(bromomethyl) derivatives provided the respective bisphosphonate esters **1**−**4** in high yields. Wittig−Horner−Emmons olefination[17] of **1**−**4** with *N*-alkylpyrrole-2-carboxaldehydes gave the corresponding bispyrroles in 52−73% yields. The all trans vinylic double bonds of **6**−**9** were confirmed by ^{1}H NMR spectral data (J = 16 Hz). ^{13}C NMR spectra and the HRMS data were in agreement with their structures. The optical and electrochemical data of **6**−**9** are shown in Table 1. These compounds showed intense absorption and fluorescence emission maxima corresponding to the $\pi-\pi^*$ transition. The time-resolved fluorescence lifetime measurements

* Corresponding authors. A.A. Fax: (+91) 471 490 186. E-mail: aajayaghosh@rediffmail.com. J.D. Fax: (+49) 941 943 4984. E-mail: joerg.daub@chemie.uni-regensburg.de.
[†] University of Regensburg.
[‡] Regional Research Laboratory, CSIR.

10.1021/ma020708t CCC: $22.00
Published on Web 9/21/2002

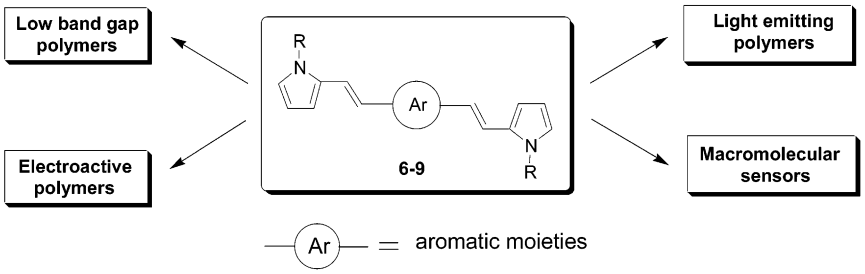

Figure 1. Conjugated bispyrroles as building blocks for novel π-conjugated polymers.

Scheme 1

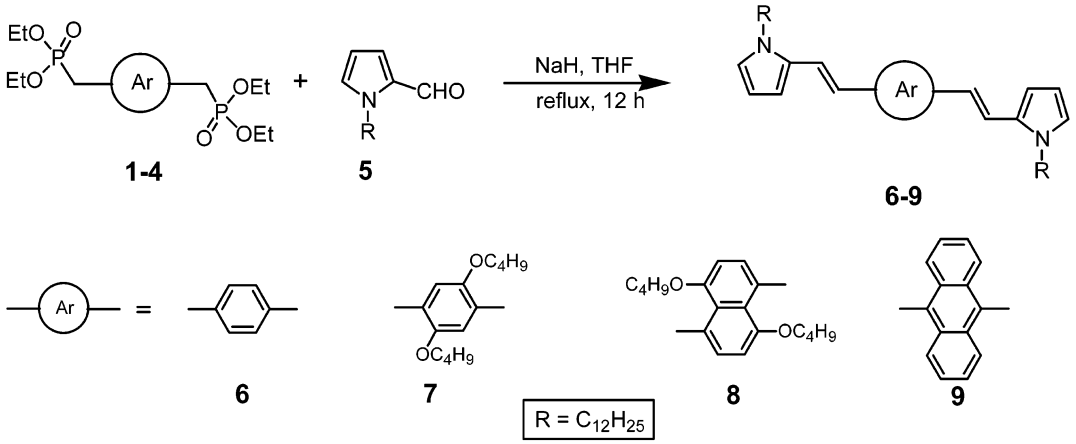

Chart 1

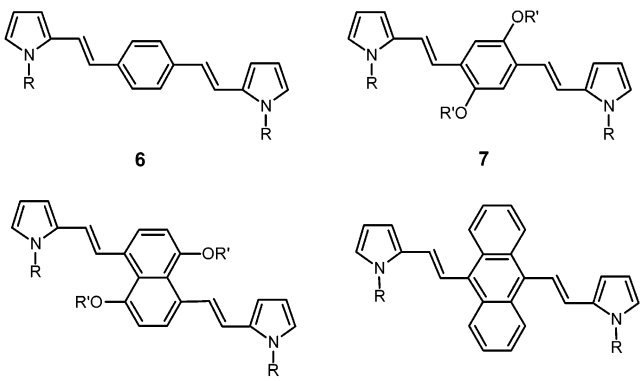

Table 1. Optical and Electrochemical Data of Bispyrroles 6−9

compound	λ_{max} (nm)[a]	λ_{em} (nm)[b]	Φ_F[c]	τ_s (ns)[d]	E_p (V)[e]
6	398	443, 471	0.32	1.06	0.37, 0.67
7	414	472	0.40	1.26	0.09, 0.60
8	375	490	0.35	2.74	0.09, 0.25
9	432	561			−0.15

[a] Absorption maxima ± 2 nm in toluene. [b] Emission maxima ± 2 nm in toluene. [c] Fluorescence quantum yields in toluene determined using quinine sulfate as standard. [d] Excited-state lifetime in toluene ±0.1 ns. [e] Peak potentials referenced vs Fc^+/Fc.

showed a single-exponential decay with lifetimes varying from 1.06 to 2.74 ns. The quantum yields of fluorescence (Φ_f) were between 0.32 and 0.4 in toluene. These findings account for a relatively planar and rigid geometry of the monomers.

Electrochemical and Spectroelectrochemical Investigation. The cyclic voltammogram (CV) of the bispyrrole **6** in dichloromethane using tetrabutylammonium hexafluorophosphate as supporting electrolyte showed two irreversible peaks at relatively low oxidation potentials when compared to that of pyrrole. For example, pyrrole has an oxidation potential of 0.9 V vs Fc^+/Fc whereas the bispyrrole **6** showed a lower oxidation potential of 0.37 and 0.67 V vs Fc^+/Fc. Upon repeated cycling of the potential, an increase in anodic and cathodic currents could be seen, which indicates the growth of a polymer film on the electrode surface (Figure 2). It is important to note that both oxidation processes have to be included in the potential cycling to obtain the polymer film. Neglecting the second oxidation presumably leads to the formation of dimers that do not deposit on the electrode. In other words, polymerization and film deposition occur only if the dimers (or oligomers) are further oxidized under the electrochemical conditions.

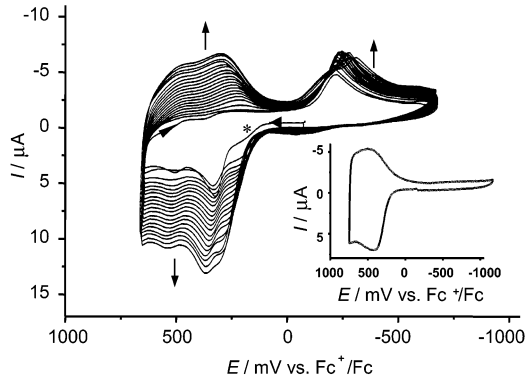

Figure 2. Multisweep CV of the bispyrrole **6** (scan rate, 100 mV/s; asterix denotes the first scan; dashed arrows give scan direction). Inset: CV of the film poly-**6** (scan rate: 25 mV/s).

The electroactivity of the electrodeposited polymer film was analyzed by the scan rate dependence of its CV. For this purpose, the working electrode was removed from the electropolymerization mixture and the

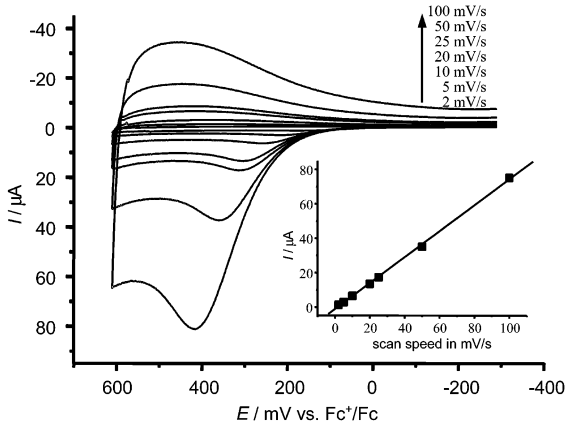

Figure 3. Scan rate dependency of the CV of poly-**6**. Inset: plot of scan speed vs anodic current for poly-**6**.

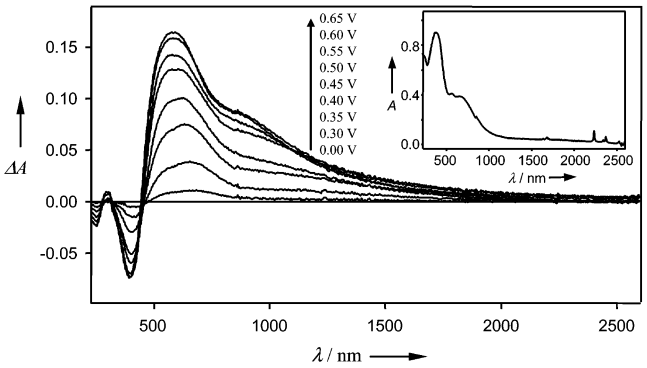

Figure 4. Spectroelectrochemical analysis of poly-**6**: spectra recorded at 0.00, 0.30, 0.35, 0.40, 0.45, 0.50, 0.55, 0.60, and 0.65 V vs Ag/AgCl pseudoreference. Inset: UV/vis/NIR spectrum of the undoped polymer.

polymer deposited electrode was thoroughly washed with dichloromethane and subsequently placed in a monomer-free electrolyte solution and its CV was recorded at various scan rates. A typical CV of the electrode-supported polymer film (poly-**6**) is shown in the inset of Figure 2. Electrochemical inactivity in the cathodic potential range is an indication that the reduction wave during polymerization is—at least in part—due to proton elimination. For a given scan rate, no change in current was detectable even after repeated scanning, indicating the reversibility of the redox processes. A plot of the anodic peak currents against the scan rates showed a linear relationship indicating that the electroactive sites are surface-bound to the platinum working electrode and that the oxidation and reduction processes are not diffusion limited (Figure 3, inset).

The change in absorption upon p-doping of the electrode-supported poly-**6** was illustrated by its spectroelectrochemical investigation in a monomer-free electrolyte solution. The polymer film was first subjected to electrochemical reduction to obtain a neutral polymer. Subsequently, the potential was increased in a stepwise manner and the UV−vis−NIR spectrum was recorded at each potential after equilibration (Figure 4). The differential absorption spectrum of the oxidized film showed the growth of a broad band with two absorption maxima around 600 (2.1 eV) and 900 nm (1.4 eV) indicating the formation of polarons.[18] The latter absorption is expected to be a valence band to the antibonding cation level transition, and the higher energy band results from the bonding to the antibonding cation level transition.[19] The reversible nature of the redox-

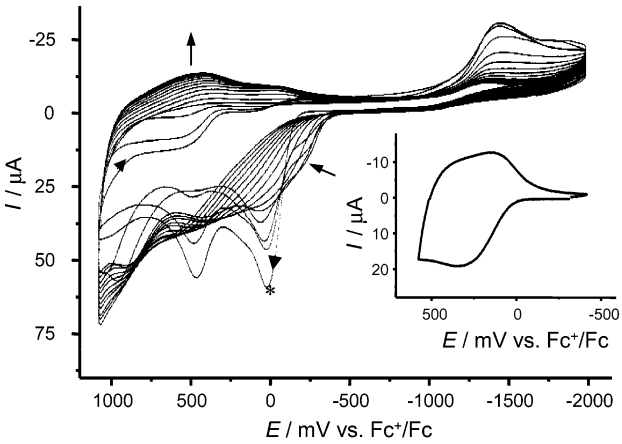

Figure 5. Multisweep CV of the bispyrrole **7** (scan rate, 500 mV/s; asterix denotes first scan, dashed arrows give scan direction). Inset: CV of the film poly-**7** (scan rate: 25 mV/s).

doping process was confirmed by restoration of the initial spectrum of the neutral film upon reduction. At higher oxidation potentials, overoxidation occurs which leads to degradation of the film. Thus, the question of a bipolaronic state of the polymer film remains unsettled. The multiple redox switching stability of poly-**6** was investigated by exposing the polymer film deposited by potential scanning on a platinum electrode, to repeated doping/dedoping processes involving about 90% of the maximum charge. For up to 2000 cycles the loss in charge was less than 5%. The excellent long-term redox switching stability of the film is an indication of its potential application in practical devices.

To study the effect of electron donating alkoxy groups on the divinylbenzene bridge, a bispyrrole **7** was prepared and subjected to multisweep cyclic voltammetry. Compound **7** in CH_2Cl_2 showed two irreversible oxidation peaks, which are lower in potential than those of **6**. The multisweep CV for the electropolymerization of **7** in CH_2Cl_2 is shown in Figure 5. Even under a high scan rate (500 mV/s) poor film formation was noticed. The retarded growth of the polymer film can be explained by the formation of highly soluble oligomers and their diffusion into the bulk solution before deposition at the electrode surface.[20] The CV of the electrodeposited polymer film in monomer-free solution is shown in the inset of Figure 5. No considerable change in the peak current could be seen even after repeated potential scanning thereby indicating a chemically reversible redox process. The scan rate dependence of the CV of poly-**7** is shown in Figure 6. In contrast to poly-**6**, the plot of the anodic peak current against the scan speed was not linear for scan speeds higher than 70 mV/s, which is a hint for suppression of diffusion of the supporting electrolyte through the polymer layer on the electrode surface.[21] The spectroelectrochemical analysis of poly-**7** in a monomer-free electrolyte solution showed a growth of a broad absorption band with two maxima at 600 (2.1 eV) and 1000 nm (1.2 eV) presumably due to polaron formation (Figure 7). It is interesting to note that the presence of the alkoxy groups in poly-**7** induce a bathochromic shift of nearly 100 nm to the long wavelength absorbing polaron band with enhanced intensity when compared to that of poly-**6**.

To investigate on the effect of different aryldivinyl-bridging moieties, bispyrroles **8** and **9** containing divinylnaphthalene and divinylanthracene moieties, respectively, were synthesized and their electrochemical

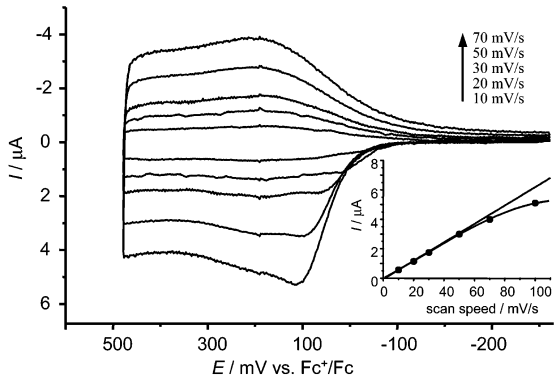

Figure 6. Scan rate dependency of the CV of poly-**7**. Inset: plot of scan speed vs anodic current for poly-**7**.

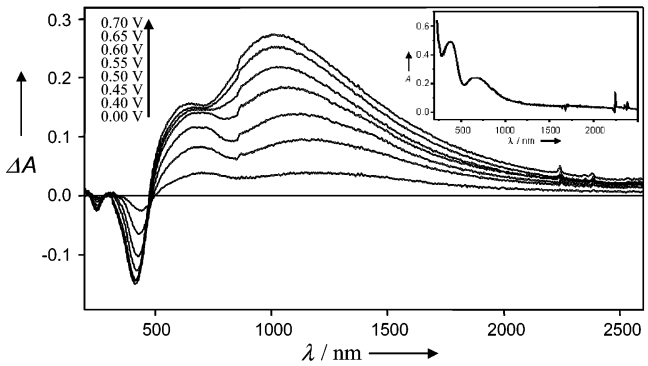

Figure 7. Spectroelectrochemical analysis of poly-**7**: spectra recorded at 0.00, 0.40, 0.45, 0.50, 0.55, 0.60, 0.65, and 0.70 V vs Ag/AgCl pseudoreference. Inset: UV/vis/NIR spectrum of the undoped polymer.

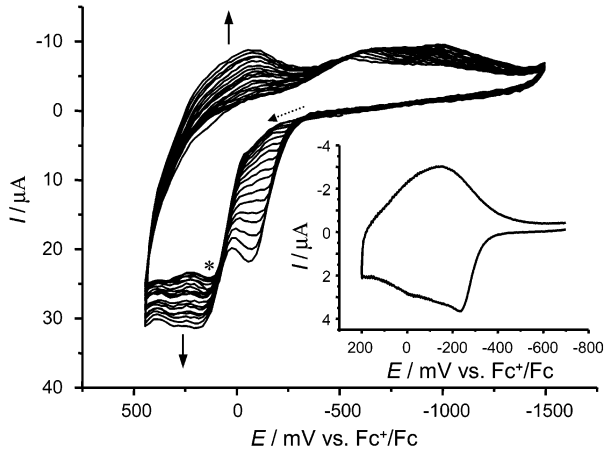

Figure 8. Multisweep CV of the bispyrrole **8** (scan rate, 250 mV/s; asterix denotes first scan, dashed arrows give scan direction). Inset: CV of the film poly-**8** (scan rate: 25 mV/s).

analyses were performed. Compound **8** showed two irreversible oxidation potentials at 0.09 and 0.25 V (vs Fc^+/Fc), which is lower than those of compounds **6** and **7**. The multisweep CV of **8** showed a growth of a polymer film on the electrode surface, at a scan rate of 250 mV/s (Figure 8). This observation reveals that the presence of alkoxy groups on the naphthalene ring has less influence on the retardation of the polymer growth when compared to that of the monomer **6**. The electrode-supported poly-**8** was relatively easier to oxidize when compared to poly-**6** and poly-**7**. Negligible decrease of the peak current after multiple charging/discharching accounts for the chemical stability of the polymer film. The CV of poly-**8** at different scan speed showed a linear

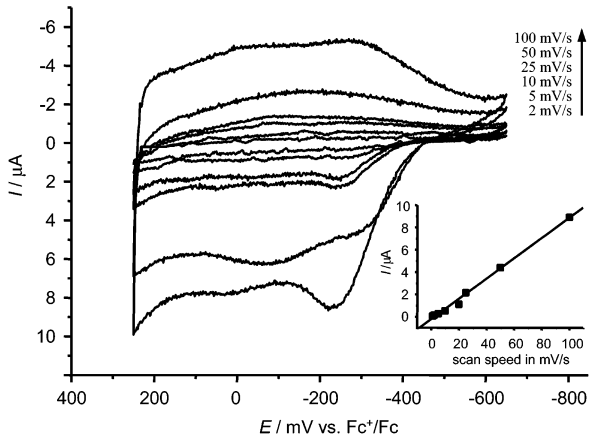

Figure 9. Scan rate dependency of the CV of poly-**8.** Inset shows the plot of scan speed vs anodic current for poly-**8**.

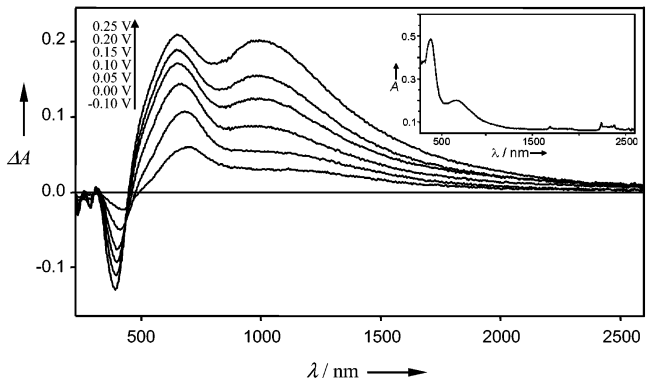

Figure 10. Spectroelectrochemical analysis of poly-**8**: spectra recorded at −0.10, 0.00, 0.05, 0.10, 0.15, 0.20, and 0.25 V vs Ag/AgCl pseudoreference. Inset: UV/vis/NIR spectrum of the undoped polymer.

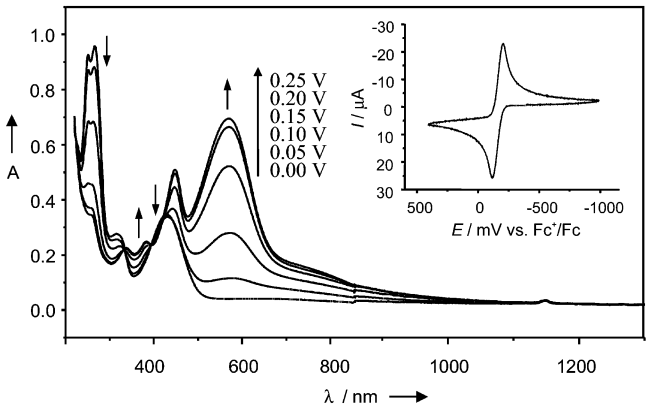

Figure 11. Spectroelectrochemical analysis of the bispyrrole **9**: spectra recorded at 0.00, 0.05, 0.1, 0.15, 0.20, and 0.25 V vs Ag/AgCl pseudoreference. Inset: CV of **9** (scan rate: 250 mV/s).

scan rate dependency against anodic current as in the case of poly-**6**, indicating the electroactivity of the polymer film (Figure 9). The spectroelectrochemical analysis of poly-**8** under different applied potential showed two clearly separated absorption maxima around 600 (2.1 eV) and 1000 nm (1.2 eV) as in the case of poly-**7** (Figure 10).

The CV of anthracene-bridged bispyrrole **9** differs significantly from pyrroles **6**−**8** (Figure 11, inset). When referenced against a weighed amount of ferrocene, the wave at −150 mV vs Fc^+/Fc accounts for a two-electron transfer, thus forming the dication in an one-step

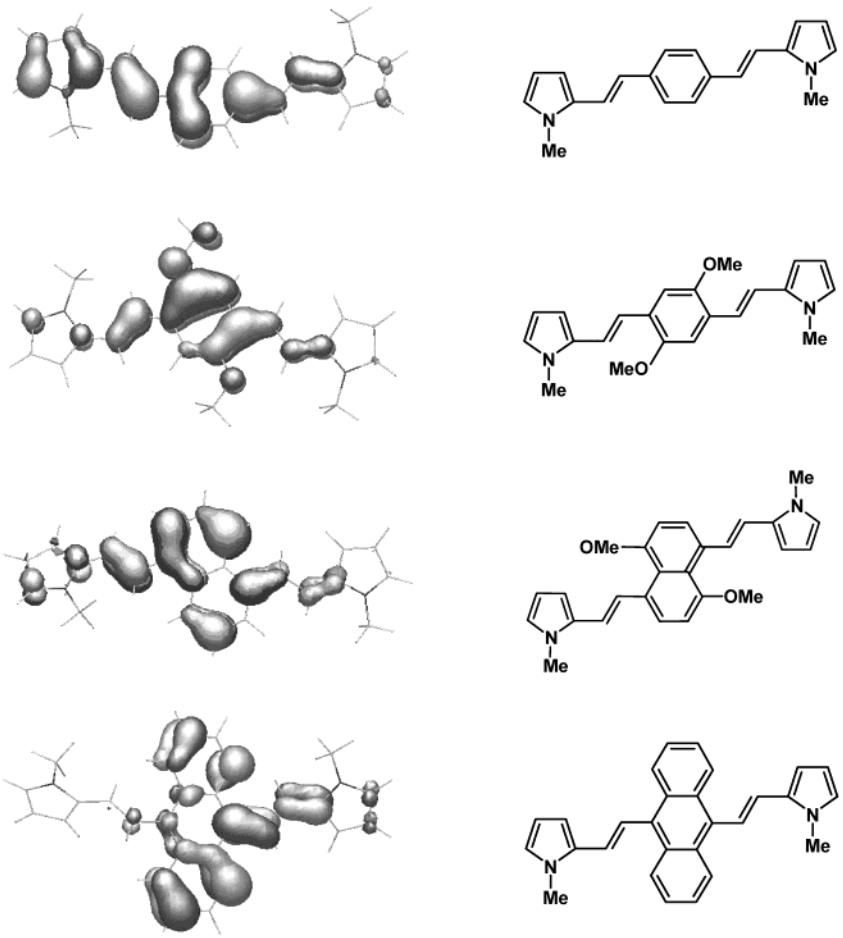

Figure 12. HOMO diagrams of $\mathbf{6}^{2+}-\mathbf{9}^{2+}$. The long hydrocarbon chains are replaced with methyl groups for simplicity.

process. Spectroelectrochemical analysis of **9** (Figure 11) has analogous features as the one reported for bis(vinyl-10*H*-phenothiazine) although its dication displays a long-wavelength absorption band at 1015 nm.[22] Upon oxidation, absorption of the neutral system at 251, 268, 310, and 410 nm were decreased, while new bands at 350, 370, 451, 577, and 750 (shoulder) nm appeared. Isosbestic points at 333, 394, and 420 nm account for a uniform process, which is completely reversible since the initial spectrum of the neutral species is restored after back reduction.

Compounds **6**−**9** constitute a class of compounds

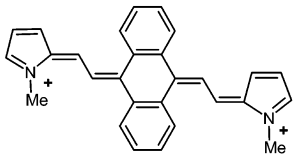

Structure 10

of the donor−bridge−donor type,[23] which are easily oxidized to radical cation and dication states. To rationalize the observed electrochemical behavior of the bispyrroles **6**−**9**, molecular properties of the doubly charged systems were calculated using semiempirical methods at AM1 level.[24] Long hydrocarbon side chains of **6**−**9** were replaced by methyl groups for simplicity. For all monomers in the dication state, the UHF (unrestricted Hartree−Fock) enthalpies of formation were lower in energy compared to the RHF (restricted Hartree−Fock), indicating the diradical character of the dications. The nearly equal charge distributions of the pyrrole moieties indicate no correlation with the propensity of film formation. In contrast, the HOMOs of $\mathbf{6}^{2+}-\mathbf{9}^{2+}$ (Figure 12) reveal considerable difference in the orbital coefficients at the C^{α}-positions of the pyrrole moieties.[25] The role of orbital coefficients at the C^{α}-positions of the pyrrole moieties in controlling the polypyrrole film formation is in accordance with the frontier molecular orbital model, that was already reported by Lacroix et al.[26] For the monomers **6** and **8**, the orbital coefficients at the α-positions of the pyrrole moieties are larger than those of **7** and **9**. Hence, the electropolymerization of these monomers is more efficient as shown by the multisweep cyclic voltammograms. On the other hand, in the case of monomer **7**, the orbital coefficient is comparatively low, and hence, the electrodeposition of the polymer film proceeds slowly. In contrast, monomer **9** has the lowest orbital coefficient and showed no tendency for polymerization. We must emphasize here that semiempirical calculations at the UHF-AM1 level allow only a qualitative estimation of the frontier orbitals. Nevertheless, the experimentally observed electropolymerization behavior of the monomers **6**−**9** could be reasonably explained by the semiempirical calculations performed at the AM1 level.

On the basis of experimental observations, a reasonable mechanism for the electropolymerization is suggested in Scheme 2, which is analogous to the mechanisms suggested earlier for other pyrrole-based monomers.[27] Upon oxidation of the monomers to their radical

Scheme 2

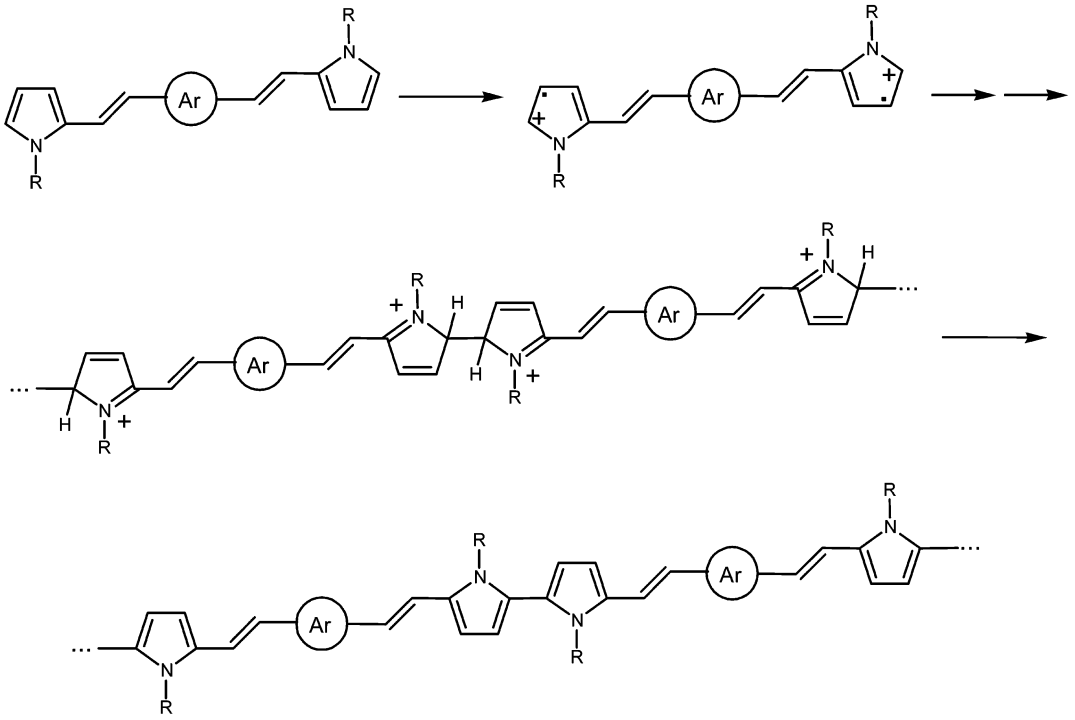

dications, oligomerization occurs depending on the orbital coefficients at the C^{α}-atoms. Subsequently, deposition of the film at the electrode surface occurs, which depends on the alkoxy chain lengths and the adjunctive diffusion properties. Finally, elimination of protons as can be seen from the reduction peak in the cyclic voltammograms, leads to the conjugated polypyrroles on the electrode. High solubility of the oligomers discourages the deposition process at a given scan speed. We have attempted the electropolymerization of a variety of monomers containing hydrocarbon side chains of varying length, all of which showed strong tendency for retarded polymerization (data not shown). In contrast to some of the earlier reports on the electrodeposition of pyrroles, addition of small amounts of water does not facilitate film formation in the present cases.[28]

Our findings reiterate that there exists a relationship between the stability of the radical cations and dications of the bispyrrole derivatives toward their electropolymerization. The electronic structure of the bridging group plays an important role in this respect. In the case of anthracene derivative **9**, the bridging group is the one that accommodates the least aromatic stabilization (resonance energy of anthracene is 0.11 eV as compared to 0.15 eV of benzene[29]). Therefore, the donor groups in **9** experience the strongest coupling, thus increasing the donor strength as indicated by the lowest oxidation potential $E_{1/2}$, which in turn is in agreement with a high-lying occupied molecular orbital (HOMO). From these considerations, the electronic structure of the dication of **9** can be represented by a quinonemethide structure **10**. The immediate formation of the dication in a one-wave−two-electron cyclic voltammogram is explained by an inversion of the oxidation potentials of the first and the second step. This merging-wave behavior can be explained by the inhibition of the electrode kinetics of the first step due to reorganization occurring upon radical cation formation.[30] This step has to overcome the anthracene aromatic stabilization and the reorganization energy resulting from planarization. The second step thereafter experiences a potential $E^{1/2}$ ($\mathbf{9}^{2+}/\mathbf{9}^{+}$), which is less positive than $E^{1/2}$ ($\mathbf{9}^{+}/\mathbf{9}$).

Conclusions

Distinctly different behaviors could be observed on the electrochemical properties of the bispyrroles **6**−**9** upon potential cycling. The electronic nature of the conjugation bridge and the alkoxy side chains play a significant role in controlling the growth of the polymer film on the electrode surface. While the bispyrroles with divinylbenzene and divinylnaphthalene bridges showed electropolymerization, the divinylanthracene-bridged bispyrrole failed to polymerize on the electrode surface. Presence of the alkoxy groups on the benzene ring has an adverse effect on the film formation. The observed electrochemical behavior of the bispyrroles **6**−**9** is rationalized on the basis of the electronic effects of the aryl bridging units, which was supported by the molecular orbital calculations. The retarded electrochemical deposition of **7** is also rationalized in terms of the higher solubility of the intermediate oligomers formed during the potential cycling. In conclusion, we have demonstrated that the electrochemical growth of a conjugated-bispyrrole-based polymer film on an electrode surface can be controlled to a large extent by the logical selection of the aryl bridging moiety and the solubility inducing alkoxy side chains.

Experimental Section

All melting points are uncorrected and were determined using a Mel-Tem-II melting point apparatus. The ^{1}H and ^{13}C NMR spectra were recorded on a 300 MHz Bruker Avance DPX spectrometer using $CDCl_3$ as solvent and tetramethylsilane as internal standard. The UV−vis−NIR spectra were recorded on a Shimadzu UV-3101 PC NIR scanning spectrophotometer. The emission spectra were measured on a Spex-Fluorolog F112X spectrofluorimeter. Fluorescence lifetimes were measured on an Edinburgh Instrument FL900CD single photon counting system. Fluorescence quantum yields were determined in toluene using quinine sulfate as standard. Cyclic

voltammetry was performed in a conventional undivided electrochemical cell with a three electrode arrangement using a computer controlled Amel 5000 or EG&G 283 system. For monomer **9**, the number of transferred electrons was determined by referencing against a known amount of added ferrocene and subsequent comparison of the areas of the cyclic voltammograms. Cyclic voltammograms of the polymer films were obtained, after thorough rinsing of the coated film with solvent and placing into a second electrochemical cell containing identical solvent and supporting electrolyte concentration, in the absence of any monomer. The UV/vis/NIR spectroelectrochemistry setup is described elsewhere.[31] Molecular orbital calculations were performed with WinMOPAC 2.0, Fujitsu Limited 1997−1998. All polymerizations were conducted under inert atmosphere (N_2) in CH_2Cl_2 and tetrabutylammonium hexafluorophosphate as supporting electrolyte (0.1 M) with a monomer concentration ranging from 10^{-4} to 10^{-3} mol L^{-1}. Potentials are referenced against ferrocenium/ferrocene redox couple. Overoxidation was avoided in all electropolymerization experiments to minimize irregular film formation due to cross-linking.

The bisphosphonate esters **1**−**4** were prepared by the reaction of the corresponding bisbromomethyl derivatives with triethyl phosphite by Michaelis-Arbuzov reaction.[16] The Wittig−Horner−Emmons[17] olefination reaction of the bisphosphonate esters **1**−**4** with *N*-dodecylpyrrole-2-carboxaldehyde provided the corresponding bispyrroles **6**−**9** in 58−73% yields, respectively.

General Procedure for the Preparation of Phosphonates (1—4). Compounds **1**−**4** were prepared by the reaction of the corresponding bisbromomethyl derivatives (10 mmol) with triethyl phosphite (5 mL) at 80 °C for 10 h followed by the removal of the unreacted triethyl phosphite under reduced pressure.

Tetraethyl[1,4-phenylenebis(methylene)]bisphosphonate (1). Yield: 95%. ^{1}H NMR ($CDCl_3$): δ 7.4 (s, 4H), 3.9−4.4 (m, 8H), 3.3 (d, J = 21.53 Hz, 4H), 1.3−1.5 (t, J = 7.2 Hz, 12H). ^{13}C NMR ($CDCl_3$): δ 129.9, 129.5, 61.75, 36.0, 29.8, 15.95.

Tetraethyl[2,5-bis(butoxy)-1,4-phenylenebis(methylene)]bisphosphonate (2). Yield: 90%. IR (neat): ν_{max} 2969, 2880, 1515, 1397, 1217, 1027, 967, 832 cm^{-1}. ^{1}H NMR ($CDCl_3$): δ 6.78 (s, 2H), 4.0−4.15 (m, 8H), 3.9−4.0 (m, 4H), 3.23 (d, J = 20.4 Hz, 4H), 1.24−1.75 (m, 20H), 0.97 (t, J = 7.4 Hz, 6H). ^{13}C NMR ($CDCl_3$): δ 150, 119.1, 114.5, 68.26, 61.52, 31.18, 26.82, 24.98, 18.94, 15.99, 13.5.

Tetraethyl[1,5-bis(butoxy)-4,8-naphthylbis(methylene)]bisphosphonate (3). Yield: 90%. ^{1}H NMR ($CDCl_3$): δ 7.26 (m, 2H), 6.81 (d, J = 8.06 Hz, 2H), 4.13 (d, J = 22.06 Hz, 4H), 4.08 (t, J = 6.2 Hz, 4H), 3.77−3.90 (m, 8H), 1.99 (m, 4H), 1.57 (m, 4H), 1.10 (t, J = 7.04 Hz, 12H), 1.4 (t, J = 7.3 Hz, 6H). ^{13}C NMR ($CDCl_3$): δ 156.14, 130.35, 126.79, 119.94, 106.36, 68.62, 61.60, 35.82, 33.99, 31.05, 19.60, 16.40, 13.97.

Tetraethyl[9,10-anthrylbis(methylene)]bisphosphonate (4). Yield: 80%. ^{1}H NMR ($CDCl_3$): δ 8.35 (dd, J = 3.23 Hz, 4H), 7.55 (d, J = 3.07 Hz, 4H), 4.2 (d, J = 20.27 Hz, 4H), 3.7−3.9 (m, 8H), 1.05 (t, J = 7.05 Hz, 12H). ^{13}C NMR ($CDCl_3$): δ 130.08, 125.53, 125.35, 124.00, 61.99, 28.04, 26.20, 16.06.

General Procedure for the Preparation of Bispyrroles (6—9). A suspension of sodium hydride (30 mmol) in THF was added slowly to a solution of the corresponding phosphonate ester (5 mmol) and *N*-dodecylpyrrole-2-carboxaldehyde (10 mmol) in THF. After refluxing for 10 h, the highly fluorescent reaction mixture was cooled and THF was removed under reduced pressure to give a solid residue. This residue was suspended in water and extracted with dichloromethane. The organic layer was washed with brine, dried over $MgSO_4$, and concentrated to give a crude product, which was further purified by several precipitations by adding methanol to a dichloromethane solution. The spectral data of **6**−**9** after recrystallization from a mixture of dichloromethane/petroleum ether were in agreement with their structures as illustrated below.

(*E*,*E*)-1,4-Bis[2-(1-dodecylpyrrol-2-yl)vinyl]benzene (6). Yield: 52%. Mp: 89−90 °C. IR: (KBr): ν_{max} 2921, 2849, 1695, 1649, 1541, 1506, 1472, 1074, 950, 689 cm^{-1}. ^{1}H NMR: ($CDCl_3$): δ 7.40 (s, 4H), 6.93 (d, J = 16.0 Hz, 2H), 6.85 (d, J = 16.0 Hz, 2H), 6.67 (s, 2H), 6.49 (m, 2H), 6.15 (t, J = 2.95 Hz, 2H), 3.95 (t, J = 7.1 MHz, 4H), 1.58−1.75 (m, 8H), 1.24−1.29 (m, 32H), 0.86 (t, J = 6.7 Hz, 6H). ^{13}C NMR: ($CDCl_3$): δ 136.78, 131.42, 126.27, 125.62, 122.68, 116.74, 108.34 106.59, 47.14, 31.99, 31.67, 29.7, 29.6, 29.41, 29.3, 26.9, 22.76, 14.1. HRMS (FAB): calcd for $C_{42}H_{64}N_2$ (M^+), 596.5070; found, 596.5089.

(*E*,*E*)-1,4-Bis[2-(1-dodecylpyrrol-2-yl)vinyl]-2,5-dibutoxybenzene (7). Yield: 58%. Mp: 79−80 °C. IR (KBr): ν_{max} 2922, 2850, 1698, 1649, 1541, 1521, 1442, 1339, 1227, 1080, 958 cm^{-1}. ^{1}H NMR ($CDCl_3$): δ 7.12 (d, J = 16.3 Hz, 2H), 7.06 (d, J = 16.3 Hz, 2H), 6.96 (s, 2H), 6.67 (s, 2H), 6.48 (m, 2H), 6.16 (t, J = 2.97 Hz, 2H), 4.02 (t, J = 6.3 Hz, 4H), 3.96 (t, J = 6.7 Hz, 4H), 1.76−1.86 (m, 8H), 1.52−1.62 (m, 8H), 1.24−1.29 (m, 32H), 1.00 (t, J = 7.16 Hz, 6H), 0.87 (t, J = 5.69 Hz, 6H). ^{13}C NMR ($CDCl_3$): δ 150.94, 132.13, 126.59, 122.41, 121.47, 117.81, 111.20, 108.15, 106.47, 69.12, 47.10, 31.89, 31.68, 31.57, 29.58, 29.31, 29.27, 26.87, 22.66, 19.47, 14.08, 13.93. HRMS: calcd for $C_{50}H_{80}N_2O_2$ (M^+), 740.6220; found, 740.6212.

(*E*,*E*)-1,5-Bis[2-(1-dodecylpyrrol-2-yl)vinyl]-4,8-dibutoxynaphthalene (8). Yield: 60%. Mp: 75−77 °C. IR: (KBr): ν_{max} 2927, 2846, 1697, 1649, 1580, 1544, 1519, 1456, 1373, 1303, 1069, 1035, 950, 774, 707 cm^{-1}. ^{1}H NMR: ($CDCl_3$): δ 8.0 (d, J = 15.5 Hz, 2H), 7.37 (d, J = 8.0 Hz, 2H), 6.85 (d, J = 7.98 Hz, 2H), 6.62 (s, 2H), 6.42 (s, 2H), 6.47 (d, J = 15.71 Hz, 2H), 6.14 (s, 2H), 4.04 (t, J = 5.97 Hz, 4H), 3.93 (t, J = 6.9 Hz, 4H), 1.74−1.83 (m, 8H), 1.23−1.47 (m, 40H), 0.80−0.87 (m, 12H). ^{13}C NMR: ($CDCl_3$): δ 156.56, 132.52, 132.0, 129.6, 126.26, 125.82, 121.31, 115.31, 107.83, 107.4, 105.19, 68.99, 47.02, 32.0, 31.75, 31.66, 29.70, 29.63, 29.42, 29.37, 26.93, 22.76, 19.74, 14.18, 13.8. HRMS (FAB): calcd $C_{54}H_{82}N_2O_2$ (M^+), 790.6376; found, 790.6404.

(*E*,*E*)-9,10-Bis[2-(1-dodecylpyrrol-2-yl)vinyl]anthracene (9). Yield: 73%. Mp: 126−127 °C. IR: (KBr): ν_{max} 2925, 2852, 1697, 1642, 1537, 1505, 1455, 1396, 1067, 958, 752 cm^{-1}. ^{1}H NMR: ($CDCl_3$): δ 8.42 (dd, J = 3.2 Hz, 4H), 7.68 (d, J = 16.20 Hz, 2H), 7.45 (dd, J = 3.2 Hz, 4H), 6.78 (d, J = 15.95 Hz, 2H), 6.76 (m, 4H), 6.27 (t, J = 2.82 Hz, 2H), 3.91 (t, J = 7.19 Hz, 4H), 1.72 (t, CH_2, 4H), 1.24−1.20 (m, CH_2, 36H), 0.86 (t, CH_3 (J = 6.96 Hz), 6H). ^{13}C NMR: ($CDCl_3$): δ 132.81, 129.67, 126.51, 126.11, 125.04, 121.91, 108.25, 106.43, 47.20, 31.87, 31.84, 29.56, 29.46, 29.29, 29.24, 26.80, 22.65, 14.09. HRMS (FAB): calcd for $C_{50}H_{68}N_2$ (M^+), 696.5383; found, 696.5377.

Acknowledgment. This is contribution number RRLT-PRU-153. We thank the Department of Science and Technology (DST), Government of India, for financial support under the Swarnajayanti Research Grant (DST/SF/C6/99-2000). Exchange visits to Germany and India, supported by DST and DAAD under the DST-DAAD-PP program and a Ph.D. fellowship from the "Studienstiftung des Deutschen Volkes" for M.B. is gratefully acknowledged. This work is part of the Graduate College "Sensory Photoreceptors" granted by the Deutsche Forschungsgemeinschaft (GRK 640/1).

References and Notes

(1) (a) Aviram, A.; Ratner, M. *Molecular Electronics: Science and Technology*; The New York Academy of Sciences: New York, 1998; Vol. 852. (b) Zerbi, G. *Organic Materials for Photonics*; Elsevier: Amsterdam, 1993. (c) Kraft, A.; Grimsdale, A. C.; Holmes, A. B. *Angew. Chem.* **1998**, *110*, 416; *Angew. Chem., Int. Ed. Engl.* **1998**, *37*, 402.

(2) (a) Bredas, J. L.; Chance, R. R. *Conjugated Polymeric Materials: Opportunities in Electronics, Optoelectronics and Molecular Electronics*; Kluwer Academic Publishers: Dordrecht, The Netherlands, 1990. (b) Müllen, K.; Wegner, G. *Electronic Materials: The Oligomer Approach*; Wiley-VCH: Weinheim, Germany, 1997. (c) Martin, R. E.; Diederich, F.

Angew. Chem., Int. Ed. **1999**, *38*, 1350. (d) Heeger, A. J. *Angew. Chem.* **2001**, *113*, 2660; *Angew. Chem., Int. Ed.* **2001**, *40*, 2591. (e) A. G. MacDiarmid, *Angew. Chem.* **2001**, *113*, 2649; *Angew. Chem., Int. Ed.* **2001**, *40*, 2581. (f) H. Shirakawa, *Angew. Chem.* **2001**, *113*, 2642; *Angew. Chem., Int. Ed.* **2001**, *40*, 2574.

(3) (a) Schöberl, U.; Salbeck, J.; Daub, J *Adv. Mater.* **1992**, *4*, 41. (b) Roncali, J. *Chem. Rev.* **1997**, *97*, 173. (c) Mohanakrishnan, A. K.; Lakshmikantham, M. V.; McDougal, C.; Cava, M. P.; Baldwin, J. W.; Metzger, R. M. *J. Org. Chem.* **1998**, *63*, 3105. (d) Dottinger, S. E.; Hohloch, M.; Segura, J. L.; Steinhuber, E.; Hanack, M.; Tompert, A.; Oelkrug, D. *Adv. Mater.* **1997**, *9*, 233. (e) Segura, J. L.; Martin, N.; Hanack, M. *Eur. J. Org. Chem.* **1999**, 643. (f) Daub, J.; Feuerer, M.; Mirlach, A.; Salbeck, J. *Synth. Met.* **1991**, *41*−*43*, 1551. (g) Mirlach, A.; Feuerer, M.; Daub, J. *Adv. Mater.* **1993**, *5*, 450. (h) Porsch, M.; Sigl-Seifert, G.; Daub, J. *Adv. Mater.* **1997**, 635. (i) Redl, F. X.; Köthe, O.; Röckl, K.; Bauer, W.; Daub, J. *Macromol. Chem. Phys.* **2000**, *201*, 2091.

(4) (a) Rudge, A.; Davey, J.; Raistrick, I.; Gottesfeld, S.; Fettaris, J. P. *J. Power Sources* **1994**, *47*, 89. (b) Arbizzani, C.; Catellani, M.; Mastragostino, M.; Mingazzani, C. *Electrochim. Acta* **1995**, *40*, 1871. (c) Hashmi, S. A.; Latham, R. J.; Linford, R. G.; Schlindwein, W. S. *Polym. Int.* **1998**, *47*, 28.

(5) Sapp, S. A.; Sotzing, G. A.; Reddinger, J. L.; Reynolds, J. R. *Adv. Mater.* **1996**, *8*, 208.

(6) (a) Diaz, A. F.; Kanazawa, K. K. *J. Chem. Soc., Chem. Commun.* **1979**, 635. (b) Kanazawa, K. K.; Diaz, A. F.; Geiss, R. H.; Gill, W. D.; Kwak, J. F.; Logan, J. A.; Rabolt, J. F.; Street, G. B. *J. Chem. Soc., Chem. Commun.* **1979**, 854. (c) Tourillon, G.; Garnier, F. *J. Electroanal. Chem.* **1982**, *135*, 173. (d) Merz, A.; Kronberger, J.; Dunsch, L.; Neudeck, A.; Petr, A.; Parkanyi, L. *Angew. Chem., Int. Ed. Engl.* **1999**, *38*, 1442. (e) Zhou, M.; Heinze, J. *J. Phys. Chem. B* **1999**, *103*, 8443. (f) Zhou, M.; Heinze, J. *J. Phys. Chem. B*, **1999**, *103*, 8451. (g) Joo, J.; Lee, J. K.; Lee, S. Y.; Jang, K. S.; Oh, E. J.; Epstein, A. J. *Macromolecules* **2000**, *33*, 5131. (h) Jerome, C.; Jerome, R. *Angew. Chem.* **1998**, *110*, 2639; *Angew. Chem., Int. Ed.* **1998**, *37*, 2488.

(7) For a recent short review on the electropolymerization of pyrrole, see: Sadki, S.; Schottland, P.; Brodie, N.; Sabouraud, G. *Chem. Soc. Rev.* **2000**, *29*, 283.

(8) Zotti, G.; Martina, S.; Wegner, G.; Schlüter, A.-D. *Adv. Mater.* **1992**, *4*, 798.

(9) (a) Reynolds, J. R.; Katritzky, A. R.; Soloducho, J.; Belyakov, S.; Sotzing, G. A.; Pyo, M. *Macromolecules* **1994**, *27*, 7225. (b) Sotzing, G. A.; Reynolds, J. R.; Katritzky, A. R.; Soloducho, J.; Belyakov, S.; Musgrave, R. *Macromolecules* **1996**, *29*, 1679. (c) Gaupp, C. L.; Zong, K.; Schottland, P.; Thompson, B. C.; Thomas, C. A.; Reynolds, J. R. *Macromolecules* **2000**, *33*, 1132. (d) Schottland, P.; Zong, K.; Gaupp, C. L.; Thompson, B. C.; Thomas, C. A.; Giurgiu, I.; Hickman, R.; Abboud, K. A.; Reynolds, J. R. *Macromolecules* **2000**, *33*, 7051.

(10) (a) Pagani, G. Berlin, A.; Canavesi, A.; Schiavon, G.; Zecchin, S.; Zotti, G. *Adv. Mater.* **1996**, *8*, 819. (b) Zotti, G.; Zecchin, S.; Schiavon, G.; Berlin, A.; Pagani, G.; Borgonovo, M.; Lazzaroni, R. *Chem. Mater.* **1997**, *9*, 2876.

(11) (a) Andrieux, C. P.; Hapiot, P.; Audebert, P.; Guyard, L.; Nguyen Dinh An, M.; Groenendaal, L.; Meijer, E. W. *Chem. Mater.* **1997**, *9*, 723. (b) Merz, A.; Schwarz, R.; Schropp, R. *Adv. Mater.* **1992**, *4*, 409. (c) Gassner, F.; Graf, S.; Merz, A. *Synth. Met.* **1997**, *87*, 75.

(12) Pyo, M.; Reynolds, J. R.; Warren, L. F.; Marcy, H. O. *Synth. Met.* **1994**, *68*, 71.

(13) (a) Ferraris, J. P.; Andrus, R. G.; Hrncir. D. C. *J. Chem. Soc., Chem. Commun.* **1989**, 1318. (b) Niziurski-Mann, R. E.; Scordilis-Kelley, C.; Liu, T.-L.; Cava, M. P.; Carlin, R. T. *J. Am. Chem. Soc.* **1993**, *115*, 887.

(14) Eldo, J.; Arunkumar, E.; Ajayaghosh, A. *Tetrahedron Lett.* **2000**, *41*, 6241.

(15) (a) Ajayaghosh, A.; Eldo, J. *Org. Lett.* **2001**, *3*, 2595. (b) Eldo, J.; Ajayaghosh, A. *Chem. Mater.* **2002**, *14*, 410.

(16) (a) Arbuzov, B. A. *Pure Appl. Chem.* **1964**, *9*, 307. (b) Stalmach, U.; Kolshorn, H.; Brehm, I.; Meier, H. *Liebigs. Ann.* **1996**, 1449.

(17) Wadsworth, W. S.; Emmons, W. D. *J. Am. Chem. Soc.* **1961**, *83*, 1733.

(18) (a) Brédas, J. L.; Scott, J. C.; Jakushi, K.; Street, G. B. *Phys. Rev. B* **1984**, *30*, 1023. (b) Brédas, J. L.; Street, G. B. *Acc. Chem. Res.* **1985**, *18*, 309. (c) Son, Y.; Rajeshwar, K. *J. Chem. Soc., Faraday Trans.* **1992**, *88*, 605. (d) van Haare, J. A. E. H.; Havinga, E. E.; Van Dongen, J. L. J.; Janssen, R. A. J.; Cornil, J.; Brédas, J.-L. *Chem. Eur. J.* **1998**, *4*, 1509.

(19) Genies, E. M.; Pernaut, J.-M. *J. Electroanal. Chem.* **1985**, *191*, 111.

(20) Benincori, T.; Brenna, E.; Sannicolò, F.; Zotti, G.; Zecchin, S.; Schiavon, G.; Gatti, C.; Frigerio, G. *Chem. Mater.* **2000**, *12*, 148.

(21) (a) Shim, Y.-B.; Park, S.-M. *J. Electrochem. Soc.* **1997**, *144*, 3027. (b) A reviewer has suggested that the nonlinearity of the scan rate dependence could also be due to the slower electron hopping within the film.

(22) (a) Knorr, A.; Daub, J. *Angew. Chem.* **1997**, *109*, 2926; *Angew. Chem., Int. Ed. Engl.* **1997**, *36*, 2817. (b) Salbeck, J.; U. Schöberl, U.; Rapp, K. M.; Daub, J. *Z. Phys. Chem.* **1991**, *171*, 191. (c) Astruc, D.; Lacoste, M.; Toupet, L. *J. Chem. Soc., Chem. Commun.* **1990**, 558. (d) Hu, K.; Evans, D. H. *J. Phys. Chem.* **1996**, *100*, 3030.

(23) (a) Büschel, M.; Helldobler, M.; Daub, J. *Chem. Commun.* **2002**, 1338. (b) Lindeman, S. V.; Rosokha, S. V.; Sun, D.; Kochi, J. K. *J. Am. Chem. Soc.* **2002**, *124*, 843.

(24) PM3 is known to give poor results for nitrogen containing systems because of overestimated charges and pyramidalization at the nitrogen atoms.

(25) In all cases the geometries and subsequently the orbitals are calculated at the UHF level, accounting for the occurrence of unpaired electrons yielding α- and β-orbitals. Only the α-orbitals are depicted. For the dications, in all cases UHF yield lower heat of formation compared to RHF.

(26) Lacroix, J.-C.; Valente, R.-J.; Maurel, F.; Lacaze, P.-C. *Chem.*—*Eur. J.* **1998**, *4*, 1667.

(27) For a detailed discussion of the polymerization mechanism, see: Heinze, J. *Top. Curr. Chem.* **1990**, *152*, 1.

(28) Zjou, M.; Heinze, J. *J. Phys. Chem. B* **1999**, *103*, 8451.

(29) Minkin, V. I.; Glukhovtsev, M. N.; Simkin, B. Y. *Aromaticity and Antiaromaticity*—*Electronical and Structural Aspects*; Wiley-Interscience: New York, 1994.

(30) Salbeck, J.; Schöberl, U.; Rapp, K. M.; Daub, J. *Z. Phys. Chem.* **1991**, *171*, 191.

(31) (a) Salbeck, J.; Aurbach, I.; Daub, J. *Dechema Monogr.* **1988**, *112*, 177; b) Salbeck, J. *J. Electroanal. Chem.* **1992**, *340*, 169. (c) Salbeck, J. *Anal. Chem.* **1993**, *65*, 2169.

MA020708T